Nuclear Engineering and Technology 54 (2022) 1644–1651

Contents lists available at ScienceDirect

Nuclear Engineering and Technology

journal homepage: www.elsevier.com/locate/net

Original Article

Adaptive second-order nonsingular terminal sliding mode power-level control for nuclear power plants

Jiuwu Hui, Jingqi Yuan*

Department of Automation, And the Key Laboratory of System Control and Information Processing/Ministry of Education, Shanghai Jiao Tong University, 800 Dongchuan Road, 200240, Shanghai, China

ARTICLE INFO

Article history:
Received 19 October 2020
Received in revised form
27 October 2021
Accepted 28 October 2021
Available online 3 November 2021

Keywords:
Nuclear power plants (NPPs)
Power-level control
Second-order nonsingular terminal sliding mode
Adaptive mechanism

ABSTRACT

This paper focuses on the power-level control of nuclear power plants (NPPs) in the presence of lumped disturbances. An adaptive second-order nonsingular terminal sliding mode control (ASONTSMC) scheme is proposed by resorting to the second-order nonsingular terminal sliding mode. The pre-existing mathematical model of the nuclear reactor system is firstly described based on point-reactor kinetics equations with six delayed neutron groups. Then, a second-order sliding mode control approach is proposed by integrating a proportional-derivative sliding mode (PDSM) manifold with a nonsingular terminal sliding mode (NTSM) manifold. An adaptive mechanism is designed to estimate the unknown upper bound of a lumped uncertain term that is composed of lumped disturbances and system states real-timely. The estimated values are then added to the controller, resulting in the control system capable of compensating the adverse effects of the lumped disturbances efficiently. Since the sign function is contained in the first time derivative of the real control law, the continuous input signal is obtained after integration so that the chattering effects of the conventional sliding mode control are suppressed. The robust stability of the overall control system is demonstrated through Lyapunov stability theory. Finally, the proposed control scheme is validated through simulations and comparisons with a proportional-integral-derivative (PID) controller, a super twisting sliding mode controller (STSMC), and a disturbance observer-based adaptive sliding mode controller (DO-ASMC).

1. Introduction

Power-level control of NPPs is a challenging task for controller designers since the dynamic model of the nuclear reactor system features inherent nonlinearity and parameters uncertainties, and the nuclear reactor system may suffer from internal and external time-varying disturbances during long-term operation [1–4]. Therefore, the power-level controller used in NPPs should have the capability not only to provide precise power-level control performance, but also to effectively reject model uncertainties and time-varying disturbances.

Owing to the simple structure, easy implementation, and mature technical analysis, the proportional-integral-derivative (PID) control method has been widely used in real-life mechanical systems. However, it is worth mentioning that the PID control cannot effectively deal with unknown model uncertainties and high-frequency disturbances. Moreover, since most parameters for the nuclear reactor system are affected by the time-varying operation conditions, the PID coefficients should be tuned online so as to improve its control performance. To this end, researchers have proposed various advanced control approaches by combining the conventional PID controller with some intelligent algorithms. For instance, Zarei et al. [5] proposed a robust PID power control approach for an innovative design of lead cooled fast reactors. In this work, the PID coefficients were calculated by utilizing a Laurent expansion scheme of the intended controller in real time. Liu et al. [6] developed a fuzzy-PID controller for power control of a nuclear reactor, in which a fuzzy logic system was exploited to tune the coefficients of the PID controller to adapt the model changing with the output power. Mousakazemi et al. [7] presented an optimized PID power controller for a pressurized water reactor. The PID coefficients were optimized and scheduled by a real-coded genetic algorithm. In addition, a number of intelligent control methods have been extensively applied in power-level control of NPPs in recent years to improve power control accuracy, while enhancing the robustness against model uncertainties and random external

* Corresponding author.
E-mail addresses: huijiuwu@sjtu.edu.cn (J. Hui), jqyuan@sjtu.edu.cn (J. Yuan).

https://doi.org/10.1016/j.net.2021.10.041

disturbances, such as model predictive control [8], observer-based control [9,10], neural network control [11], fuzzy logical control [12,13], fault tolerated intelligent control [14], and sliding mode control (SMC) [15–17].

The aforementioned control methods have their own advantages and disadvantages. For the SMC approach, its characteristics, such as strong robustness against external disturbances and insensitivity to parameter uncertainties, make designing a controller for power-level control of NPPs more effective. In Ref. [15], a discrete-time output feedback sliding mode control strategy was developed for spatial power control of a large pressurized heavy water reactor, where the system outputs were the 14 zonal power levels. In Ref. [16], a fractional-order sliding mode controller was designed based on a nonlinear fractional-order model of the nuclear reactor system, which was capable of tracking the reference power trajectory and overcoming uncertainties and external disturbances simultaneously. By virtue of sliding mode control techniques, Wang et al. [17] proposed a nonlinear power-level tracking controller for a modular high-temperature gas-cooled nuclear reactor (MHTGR), where an adaptive algorithm was added to the proposed control law to reduce the chattering phenomenon associated with SMC. Unfortunately, the aforementioned SMC schemes can only guarantee asymptotic stability of the control system, as they were all designed using linear sliding mode manifolds, which implies that the control error between the desired power and the actual one converges to zero in an infinite time.

In order to achieve better transient response and finite-time convergence of the SMC systems, terminal sliding mode control (TSMC) approach has been proposed in the literature [18,19] via the nonlinear sliding mode manifold. Furthermore, nonsingular terminal sliding mode control approach has also been developed to overcome the singular problem existing in TSMC [20,21]. Inspired by the foregoing observations, an adaptive second-order nonsingular terminal sliding mode control (ASONTSMC) scheme is proposed for NPPs subject to model uncertainties and external disturbances in this paper. The pre-existing mathematical model of nuclear reactor system is firstly described, and then a second-order nonsingular terminal sliding mode manifold is designed via a proportional-derivative sliding mode (PDSM) manifold and a nonsingular terminal sliding mode (NTSM) manifold. In addition, an adaptive mechanism is introduced to estimate the unknown upper bound of the system uncertainties online, where the estimated values are used in the control law for compensating the adverse effects of disturbances. Unlike previous work [17] in which an adaptive algorithm was introduced to reduce the chattering phenomenon associated with the SMC at the price of deteriorating control performance, the discontinuous term is contained in the first time derivative of the actual control input in this paper, meaning that the continuous control input is obtained after integration such that the chattering effects are considerably eliminated without degrading system robustness. Finally, comparative simulation results between the proposed ASONTSMC scheme and some existing controllers are presented to validate the feasibility and superiority of the proposed control scheme.

The rest of this paper is organized as follows. In Section 2, the mathematical model of the nuclear reactor system is described. In Section 3, an ASONTSMC scheme is proposed for power-level control of NPPs. To demonstrate the effectiveness of the proposed control scheme, comparative simulation results are presented in Section 4. Section 5 draws the conclusions.

2. Mathematical model of nuclear reactor system

In this section, the pre-existing mathematical model of the nuclear reactor system, which consists of point-reactor kinetics equations with six delayed neutron groups, output power equation, fuel and coolant thermal-hydraulics equations, and total reactivity equation, is described at first. After that, the control objective of this study is described.

The point-reactor kinetics equations have been commonly employed in the field of nuclear engineering, e.g., dynamical modeling and simulation for a MHTGR [22–24], estimation of poisons reactivity [25], stability analysis of a reactor with power reactivity feedback [26], the study of maximal speed of control rods for a water-water energetic reactor (WWER)-1000 nuclear reactor [27], power-level control [28–31], and so on. The point-reactor kinetics equations are given as [32,33]

$$\frac{\mathrm{d}n_r}{\mathrm{d}t} = \frac{\rho-\beta}{\Lambda}n_r + \sum_{i=1}^{6}\frac{\beta_i}{\Lambda}c_{ri} + d \tag{1}$$

$$\frac{\mathrm{d}c_{ri}}{\mathrm{d}t} = \lambda_i n_r - \lambda_i c_{ri} \tag{2}$$

where n_r and c_{ri} denote the relative neutron density and the relative density of the ith group precursor, respectively, Λ, β_i, and λ_i denote the prompt neutron life time, the decay constant of the ith group neutron precursor, and the ith group delayed neutron fraction, respectively, ρ denotes the total reactivity, and d denotes the lumped disturbances which consists of model uncertainties, unmodeled dynamics, and unknown external time-varying disturbances.

The total reactivity is composed of reactivity due to control rod movement, fuel and coolant temperature reactivities, which can be expressed as

$$\rho = \rho_r + \alpha_f(T_f - T_{f0}) + \frac{\alpha_c}{2}(T_l - T_{l0}) + \frac{\alpha_c}{2}(T_e - T_{e0}) \tag{3}$$

$$\frac{\mathrm{d}\rho_r}{\mathrm{d}t} = G_r Z_r \tag{4}$$

where ρ_r, Z_r, and G_r denote the control rod reactivity, the control rod speed, and the reactivity worth of the rod per unit length, respectively, T_f, T_l, and T_e denote the fuel temperature, the temperature of the coolant leaving the reactor, and the temperature of the coolant entering the reactor, respectively, T_{f0}, T_{l0}, and T_{e0} denote the initial equilibrium fuel temperature, the temperature of the coolant leaving the reactor, and the temperature of the coolant entering the reactor, respectively, and α_f and α_c denote the fuel and the coolant temperature reactivity coefficient, respectively.

On the basis of the law of energy conservation, the fuel and coolant thermal-hydraulics equations are given as

$$\frac{\mathrm{d}T_f}{\mathrm{d}t} = \frac{f_f P_0}{\mu_f}n_r - \frac{\Omega}{\mu_f}T_f + \frac{\Omega}{2\mu_f}T_l + \frac{\Omega}{2\mu_f}T_e \tag{5}$$

$$\frac{\mathrm{d}T_l}{\mathrm{d}t} = \frac{(1-f_f)P_0}{\mu_c}n_r + \frac{\Omega}{\mu_c}T_f - \frac{2M+\Omega}{2\mu_c}T_l + \frac{2M-\Omega}{2\mu_c}T_e \tag{6}$$

where P_0 denotes the nominal reactor output power, f_f denotes the fraction of reactor power deposited in the fuel, M denotes the mass flow rate multiplied by heat capacity of the coolant, Ω denotes the heat transfer coefficient between fuel and coolant, and μ_f and μ_c

denote the total heat capacity of the fuel and coolant, respectively.

Then, the reactor output power is given as

$$P = P_0 n_r \tag{7}$$

The control object in this study is to design an ASONTSMC scheme for the NPP in the presence of unknown time-varying lumped disturbances such that the output power P of the nuclear reactor system converges to the desired one precisely. Before the ASONTSMC scheme formulation, the following mild assumptions are imposed.

Assumption 2.1. The lumped disturbances d and its first and second time derivatives are unknown but bounded.

Assumption 2.2. The desired power P_d and its first, second, and third time derivatives are known and bounded.

3. ASONTSMC scheme design

This section presents the adaptive second-order nonsingular terminal sliding mode power-level control scheme for the NPP. Firstly, define the power error as follows:

$$e_p = P - P_d \tag{8}$$

Differentiating the power control error e_p with respect to time, the first, second, and third derivatives are expressed as

$$\begin{cases} \dot{e}_p = \dot{P} - \dot{P}_d \\ \quad = P_0\left(\dfrac{\rho-\beta}{\Lambda}n_r + \sum_{i=1}^{6}\dfrac{\beta_i}{\Lambda}c_{ri} + d\right) - \dot{P}_d \\ \ddot{e}_p = P_0\left(\dfrac{\rho-\beta}{\Lambda}\dot{n}_r + \dfrac{\dot{\rho}}{\Lambda}n_r + \sum_{i=1}^{6}\dfrac{\beta_i}{\Lambda}\dot{c}_{ri} + \dot{d}\right) - \ddot{P}_d \\ e_p = P_0\left(\dfrac{2\dot{\rho}}{\Lambda}\dot{n}_r + \dfrac{\rho-\beta}{\Lambda}\ddot{n}_r + \dfrac{\ddot{\rho}}{\Lambda}n_r + \sum_{i=1}^{6}\dfrac{\beta_i}{\Lambda}\ddot{c}_{ri} + \ddot{d}\right) - P_d \end{cases} \tag{9}$$

where $\ddot{\rho}$ is expressed as

$$\ddot{\rho} = G_r\dot{Z}_r + \alpha_f\ddot{T}_f + \frac{\alpha_c}{2}\ddot{T}_l \tag{10}$$

Then, the following linear PDSM manifold is constructed:

$$s_p = k_1\dot{e}_p + k_2 e_p \tag{11}$$

where k_1 and k_2 are positive design parameters to be determined later. Differentiating equation (11) with respect to time, and substituting equation (9) into it yields

$$\begin{aligned} \dot{s}_p &= k_1\ddot{e}_p + k_2\dot{e}_p \\ &= k_1P_0\left(\frac{\rho-\beta}{\Lambda}\dot{n}_r + \frac{\dot{\rho}}{\Lambda}n_r + \sum_{i=1}^{6}\frac{\beta_i}{\Lambda}\dot{c}_{ri} + \dot{d}\right) - k_1\ddot{P}_d \\ &\quad + k_2P_0\left(\frac{\rho-\beta}{\Lambda}n_r + \sum_{i=1}^{6}\frac{\beta_i}{\Lambda}c_{ri} + d\right) - k_2\dot{P}_d \end{aligned} \tag{12}$$

Next, differentiating equation (12) with respect to time, and substituting equation (9) into it yields

$$\begin{aligned} \ddot{s}_p &= k_1e_p + k_2\ddot{e}_p \\ &= k_1P_0\left(\frac{2\dot{\rho}}{\Lambda}\dot{n}_r + \frac{\rho-\beta}{\Lambda}\ddot{n}_r + \frac{\ddot{\rho}}{\Lambda}n_r + \sum_{i=1}^{6}\frac{\beta_i}{\Lambda}\ddot{c}_{ri} + \ddot{d}\right) - k_1P_d \\ &\quad + k_2P_0\left(\frac{\rho-\beta}{\Lambda}\dot{n}_r + \frac{\dot{\rho}}{\Lambda}n_r + \sum_{i=1}^{6}\frac{\beta_i}{\Lambda}\dot{c}_{ri} + \dot{d}\right) - k_2\ddot{P}_d \\ &= \frac{k_1P_0G_r\dot{Z}_r}{\Lambda}n_r - k_1P_d - k_2\ddot{P}_d + F \end{aligned} \tag{13}$$

where F represents the lumped uncertain term defined as

$$\begin{aligned} F &= k_1P_0\left(\frac{2\dot{\rho}}{\Lambda}\dot{n}_r + \frac{\rho-\beta}{\Lambda}\ddot{n}_r + \frac{\alpha_f\ddot{T}_f + \frac{\alpha_c}{2}\ddot{T}_l}{\Lambda}n_r + \sum_{i=1}^{6}\frac{\beta_i}{\Lambda}\ddot{c}_{ri} + \ddot{d}\right) \\ &\quad + k_2P_0\left(\frac{\rho-\beta}{\Lambda}\dot{n}_r + \frac{\dot{\rho}}{\Lambda}n_r + \sum_{i=1}^{6}\frac{\beta_i}{\Lambda}\dot{c}_{ri} + \dot{d}\right) \\ &= a_0 + a_1Z_r + a_2T_f + a_3T_l + a_4c_r + a_5n_r \end{aligned} \tag{14}$$

where $a_0, a_1, a_2\, a_3, a_4, a_5$ are unknown and bounded terms, and $c_r = (\beta_1c_{r1} + \beta_2c_{r2} + \beta_3c_{r3} + \beta_4c_{r4} + \beta_5c_{r5} + \beta_6c_{r6})/(\beta_1 + \beta_2 + \beta_3 + \beta_4 + \beta_5 + \beta_6)$.

To guarantee that s_p converges to zero in a finite time, the following NTSM manifold is designed by combining the PDSM manifold:

$$\sigma_p = s_p + c|\dot{s}_p|^{\frac{p}{q}}\mathrm{sign}(\dot{s}_p) \tag{15}$$

where $c > 0$ is a design parameter, and p and q are positive odd integers satisfying $1 < p/q < 2$.

Supposing that the NTSM manifold σ_p reaches zero in a finite time t_σ, i.e., $\sigma_p(t_\sigma) = 0$, the NTSM manifold can be rewritten as

$$s_p + c|\dot{s}_p|^{\frac{p}{q}}\mathrm{sign}(\dot{s}_p) = 0 \tag{16}$$

The finite time t_s from both $s_p(t_\sigma) \neq 0$ and $\dot{s}_p(t_\sigma) \neq 0$ to $s_p(t_\sigma + t_s) = 0$ and $\dot{s}_p(t_\sigma + t_s) = 0$ is obtained as [20]

$$t_s = \frac{pc^{-\frac{p}{q}}}{p-q}|s(t_\sigma)|^{1-\frac{q}{p}} \tag{17}$$

When the PDSM manifold s_p reaches zero at the instant $t = t_\sigma + t_s$, the dynamics of the nuclear reactor system is determined by the following first-order linear differential equation:

$$k_1\dot{e}_p + k_2e_p = 0 \tag{18}$$

By solving the first-order linear differential equation (18), we have

$$e_p = e_p(t_\sigma + t_s)e^{-\frac{k_2}{k_1}(t-t_\sigma-t_s)} \tag{19}$$

from which it can be concluded that the power control error e_p will exponentially converge to zero, and the convergence rate is determined by the gains k_1 and k_2, where a larger gain k_2 and a smaller gain k_1 will lead to faster convergence of the power error e_p. However, the gain k_2 cannot be arbitrarily large, and the gain k_1

cannot be arbitrarily small due to the physical limitation of the control rod speed. This indicates that the gains k_1 and k_2 should be suitably chosen to make a trade-off between the actuator limitation and the convergence rate of the power error e_p.

In the following, the control task is to design control input Z_r such that the NTSM manifold σ_p reaches zero in a finite time. Differentiating σ_p with respect to time, and substituting equations (10) and (13) into it yields

$$\begin{aligned}\dot{\sigma}_p &= \dot{s}_p + \frac{cp}{q}|\dot{s}_p|^{\frac{p}{q}-1}\ddot{s}_p \\ &= \frac{cp}{q}|\dot{s}_p|^{\frac{p}{q}-1}\left(\ddot{s}_p + \frac{q}{cp}|\dot{s}_p|^{2-\frac{p}{q}}\mathrm{sign}(\dot{s}_p)\right) \\ &= \frac{cp}{q}|\dot{s}_p|^{\frac{p}{q}-1}\left(\frac{k_1P_0G_r\dot{Z}_r}{\Lambda}n_r - k_1P_d - k_2\ddot{P}_d + F + \frac{q}{cp}|\dot{s}_p|^{2-\frac{p}{q}}\mathrm{sign}(\dot{s}_p)\right)\end{aligned} \tag{20}$$

In this paper, the control input Z_r that consists of an equivalent control law Z_{re} and a reaching law Z_{rs} is designed as

$$Z_r = Z_{re} + Z_{rs} = \int_0^t \left(\dot{Z}_{re} + \dot{Z}_{rs}\right)d_\tau \tag{21}$$

where the term $\dot{Z}_{re}$ is designed to cancel out the additional terms of $\dot{\sigma}_p$, and the term $\dot{Z}_{rs}$ is introduced to deal with disturbances and render the system converge to the NTSM manifold σ_p in a finite time. Let the right-hand side of equation (21) be zero, i.e., $\dot{\sigma}_p = 0$, the first time derivative of the equivalent control law can be obtained as

$$\dot{Z}_{re} = -\frac{\Lambda}{k_1P_0G_rn_r}\left(k_1P_d + k_2\ddot{P}_d - \frac{q}{cp}|\dot{s}_p|^{2-\frac{p}{q}}\mathrm{sign}(\dot{s}_p)\right) \tag{22}$$

Substituting equations (21) and (22) into equation (20), one has

$$\dot{\sigma}_p = \frac{cp}{q}|\dot{s}_p|^{\frac{p}{q}-1}\left(\frac{k_1P_0G_rn_r\dot{Z}_{rs}}{\Lambda} + F\right) \tag{23}$$

To proceed with the design of the control term $\dot{Z}_{rs}$, the following assumption is needed.

Assumption 3.1. The unknown lumped uncertain term F is bounded by

$$|F| < v_0 + v_1|Z_r| + v_2T_f + v_3T_l + v_4c_r + v_5n_r \tag{24}$$

where v_0, v_1, v_2, v_3, v_4, and v_5 are unknown positive constants.

It should be noted that the upper bound of the lumped uncertain term F is difficult to determined in practical applications due to the time-varying external environment and operating conditions. On the other hand, the overestimated upper bound may result in excessive control inputs, thus an adaptive mechanism is introduced to estimate the upper bound of the uncertain term F herein, in which the adaptation laws are designed as follows:

$$\begin{cases}\dot{\hat{v}}_0 = \kappa_0\dfrac{cp}{q}|\dot{s}_p|^{\frac{p}{q}-1}\sigma_p\mathrm{sat}(\sigma_p) \\ \dot{\hat{v}}_1 = \kappa_1\dfrac{cp}{q}|\dot{s}_p|^{\frac{p}{q}-1}\sigma_p\mathrm{sat}(\sigma_p)|Z_r| \\ \dot{\hat{v}}_2 = \kappa_2\dfrac{cp}{q}|\dot{s}_p|^{\frac{p}{q}-1}\sigma_p\mathrm{sat}(\sigma_p)T_f \\ \dot{\hat{v}}_3 = \kappa_3\dfrac{cp}{q}|\dot{s}_p|^{\frac{p}{q}-1}\sigma_p\mathrm{sat}(\sigma_p)T_l \\ \dot{\hat{v}}_4 = \kappa_4\dfrac{cp}{q}|\dot{s}_p|^{\frac{p}{q}-1}\sigma_p\mathrm{sat}(\sigma_p)c_r \\ \dot{\hat{v}}_5 = \kappa_5\dfrac{cp}{q}|\dot{s}_p|^{\frac{p}{q}-1}\sigma_p\mathrm{sat}(\sigma_p)n_r\end{cases} \tag{25}$$

where $\hat{v}_i$ $(i = 0, 1, 2, 3, 4, 5)$ represent the estimations of v_i $(i = 0, 1, 2, 3, 4, 5)$, $\kappa_i > 0$ $(i = 0, 1, 2, 3, 4, 5)$ are design parameters that determine the rate of adaptation, and $\mathrm{sat}(\sigma_p)$ represents the saturation function defined as

$$\mathrm{sat}(\sigma_p) = \begin{cases}\dfrac{\sigma_p}{\Delta}, & if\ |\sigma_p| \le \Delta \\ \mathrm{sign}(\sigma_p), & if\ |\sigma_p| > \Delta\end{cases} \tag{26}$$

where Δ represents the thickness of the boundary layer. In addition, $\hat{v}_i(0)$ and κ_i $(i = 0, 1, 2, 3, 4, 5)$ are suitably chosen such that $\hat{v}_i - v_i \ge 0$ $(i = 0, 1, 2, 3, 4)$ and $\hat{v}_5 - v_5 > 0$. The control term $\dot{Z}_{rs}$ is designed as

$$\begin{aligned}\dot{Z}_{rs} &= -\frac{\Lambda}{k_1P_0G_rn_r}\Big(k_3\mathrm{sat}(\sigma_p) \\ &\quad + \left(\hat{v}_0 + \hat{v}_1|Z_r| + \hat{v}_2T_f + \hat{v}_3T_l\right. \\ &\quad \left. + \hat{v}_4c_r + \hat{v}_5n_r\right)\mathrm{sat}(\sigma_p)\Big) \\ &= -\frac{\Lambda}{k_1P_0G_rn_r}\left(k_3\mathrm{sat}(\sigma_p) + \bar{F}\mathrm{sat}(\sigma_p)\right)\end{aligned} \tag{27}$$

where $\bar{F}$ represents the estimated upper bound of the lumped uncertain term F, that is, $\bar{F} = \hat{v}_0 + \hat{v}_1|Z_r| + \hat{v}_2T_f + \hat{v}_3T_l + \hat{v}_4c_r + \hat{v}_5n_r$, and k_3 is a positive constant to be determined later.

Consider the following Lyapunov function candidate:

$$V = \frac{1}{2}\sigma_p^2 + \sum_0^5 \frac{1}{2\kappa_i}\tilde{v}_i^2 \tag{28}$$

where $\tilde{v}_i = v_i - \hat{v}_i$ $(i = 0, 1, 2, 3, 4, 5)$. Differentiating the Lyapunov function (28) with respect to time, and substituting equations (23)–(25) and (27) into it yields

$$\begin{aligned}\dot{V} &= \sigma_p\dot{\sigma_p} - \sum_0^5 \frac{1}{K_i}\tilde{v}_i\dot{\hat{v}}_i \\ &= \frac{\sigma_p cp}{q}|\dot{s}_p|^{\frac{p}{q}-1}\left(\frac{k_1P_0G_rn_r\dot{Z}_{rs}}{\Lambda}+F\right) - \sum_0^5 \frac{1}{K_i}\tilde{v}_i\dot{\hat{v}}_i \\ &< -\frac{cpk_3}{q}|\dot{s}_p|^{\frac{p}{q}-1}\sigma_p\mathrm{sat}(\sigma_p) \\ &+\frac{cp}{q}|\dot{s}_p|^{\frac{p}{q}-1}\sigma_p\mathrm{sat}(\sigma_p)\Big((v_0+v_1|Z_r|+v_2T_f+v_3T_l+v_4c_r+v_5n_r) \\ &-(\hat{v}_0+\hat{v}_1|Z_r|+\hat{v}_2T_f+\hat{v}_3T_l+\hat{v}_4c_r+\hat{v}_5n_r)\Big) - \sum_0^5 \frac{1}{K_i}\tilde{v}_i\dot{\hat{v}}_i \\ &= -\frac{cpk_3}{q}|\dot{s}_p|^{\frac{p}{q}-1}\sigma_p\mathrm{sat}(\sigma_p) \le 0\end{aligned} \tag{29}$$

Next, define the following Lyapunov function candidate:

$$V_0 = \frac{1}{2}\sigma_p^2 \tag{30}$$

From equation (28), the first time derivative of the Lyapunov function candidate (30) can be obtained as

$$\begin{aligned}\dot{V}_0 &= \dot{V} + \sum_0^5 \frac{1}{K_i}\tilde{v}_i\dot{\hat{v}}_i \\ &\le -\frac{cpk_3}{q}|\dot{s}_p|^{\frac{p}{q}-1}\sigma_p\mathrm{sat}(\sigma_p) + \sum_0^5 \frac{1}{K_i}\tilde{v}_i\dot{\hat{v}}_i\end{aligned} \tag{31}$$

It can be observed from equation (25) that the adaptation laws $\dot{\hat{v}}_i \ge 0$ $(i = 0,1,2,3,4,5)$. In the case of $\tilde{v}_i \le 0$ $(i = 0,1,2,3,4,5)$, i.e., $v_i \le \hat{v}_i$ $(i = 0,1,2,3,4,5)$, one has $\sum_0^5 \frac{1}{K_i}\tilde{v}_i\dot{\hat{v}}_i \le 0$, which yields

$$\dot{V}_0 \le -\frac{cpk_3}{q}|\dot{s}_p|^{\frac{p}{q}-1}\sigma_p\mathrm{sat}(\sigma_p) \tag{32}$$

In the case of $\tilde{v}_i > 0$ $(i = 0,1,2,3,4,5)$, i.e., $v_i > \hat{v}_i$ $(i = 0,1,2,3,4,5)$, one gets $\dot{\hat{v}}_i \ge 0$ $(i = 0,1,2,3,4,5)$ hold, then it follows that $\hat{v}_i$ will rise to v_i in a finite time T_i if $\dot{\hat{v}}_i > 0$, that is, $\tilde{v}_i(T_i) = v_i(T_i) - \hat{v}_i(T_i) = 0$. For the case of $\dot{\hat{v}}_i = 0$, one has $\tilde{v}_i\dot{\hat{v}}_i = 0$, meaning that the inequality (32) can also be obtained. In addition, for the cases of $\tilde{v}_i > 0$ and $\tilde{v}_j \le 0$ $(i \ne j)$, the analysis follows the above two cases, and the inequality (32) can also be obtained.

As a result, there always exists a finite time T such that

$$\dot{V}_0 \le -\frac{cpk_3}{q}|\dot{s}_p|^{\frac{p}{q}-1}\sigma_p\mathrm{sat}(\sigma_p) \le -\frac{\sqrt{2}cpk_3}{q}|\dot{s}_p|^{\frac{p}{q}-1}V_0^{\frac{1}{2}},\ t > T \tag{33}$$

For the case of $\dot{s}_p \ne 0$, it is obtained from inequality (33) that the NTSM manifold $\sigma_p = 0$ can be reached in a finite time according to the Lyapunov stability theory [34].

For the case of $\dot{s}_p = 0$, substituting control terms (22) and (27) into equation (13) yields

$$\begin{aligned}\ddot{s}_p \le\ & v_0 + v_1Z_r + v_2T_f + v_3T_l + v_4c_r + v_5n_r \\ & -(\hat{v}_0 + \hat{v}_1|Z_r| + \hat{v}_2T_f + \hat{v}_3T_l + \hat{v}_4c_r + \hat{v}_5n_r)\mathrm{sat}(\sigma_p) - k_3\mathrm{sat}(\sigma_p)\end{aligned} \tag{34}$$

Since a_i $(i = 0, 1, 2, 3, 4, 5)$ are unknown terms, one can suitably choose $\hat{v}_i(0)$ and κ_i $(i = 0, 1, 2, 3, 4, 5)$ to satisfy

$$\hat{v}_0 - v_0 = \hat{v}_0(0) + \int_0^t \kappa_0\frac{cp}{q}|\dot{s}_p|^{\frac{p}{q}-1}\sigma_p\mathrm{sat}(\sigma_p)d_\tau - v_0 \ge 0 \tag{35}$$

$$\hat{v}_1 - v_1 = \hat{v}_1(0) + \int_0^t \kappa_1\frac{cp}{q}|\dot{s}_p|^{\frac{p}{q}-1}\sigma_p\mathrm{sat}(\sigma_p)|Z_r|d_\tau - v_0 \ge 0 \tag{36}$$

$$\hat{v}_2 - v_3 = \hat{v}_2(0) + \int_0^t \kappa_2\frac{cp}{q}|\dot{s}_p|^{\frac{p}{q}-1}\sigma_p\mathrm{sat}(\sigma_p)T_fd_\tau - v_0 \ge 0 \tag{37}$$

$$\hat{v}_3 - v_3 = \hat{v}_3(0) + \int_0^t \kappa_3\frac{cp}{q}|\dot{s}_p|^{\frac{p}{q}-1}\sigma_p\mathrm{sat}(\sigma_p)T_ld_\tau - v_0 \ge 0 \tag{38}$$

$$\hat{v}_4 - v_4 = \hat{v}_4(0) + \int_0^t \kappa_4\frac{cp}{q}|\dot{s}_p|^{\frac{p}{q}-1}\sigma_p\mathrm{sat}(\sigma_p)c_rd_\tau - v_0 \ge 0 \tag{39}$$

$$\hat{v}_5 - v_5 = \hat{v}_5(0) + \int_0^t \kappa_5\frac{cp}{q}|\dot{s}_p|^{\frac{p}{q}-1}\sigma_p\mathrm{sat}(\sigma_p)n_rd_\tau - v_0 > 0 \tag{40}$$

For the cases of $\sigma_p > 0$ and $\sigma_p < 0$, it follows from equation (34) and Assumption 3 that $\ddot{s}_p < -k_3$ and $\ddot{s}_p > k_3$ hold, respectively, meaning that $\dot{s}_p = 0$ is not an attractor with respect to the NTSM manifold σ_p. Hence, it can be concluded from the above analysis that the NTSM manifold $\sigma_p = 0$ can be reached from anywhere in a finite time. As previously discussed, if the manifold $\sigma_p = 0$ is reached at the instant $t = t_\sigma$, then the PDSM manifold $s_p = 0$ would be reached at the instant $t = t_\sigma + t_s$, and finally the power control error would exponentially converge to zero.

Remark 3.1. Compared with the published SMC schemes [35,36], this work copes with the lumped disturbances using an adaptive mechanism that does not require the prior knowledge of the lumped disturbances.

Remark 3.2. It is well known that the chattering phenomenon due to discontinuous high-frequency switching control associated with the conventional SMC is the greatest barrier in practical implementations, which may damage control devices, excite unmodeled system dynamics, lead to control performance degradation and even cause instability of the systems. In literature, a variety of methods have been proposed to suppress the chattering phenomenon, such as the boundary layer SMC, the novel reaching laws, and the disturbance observer-based SMC [37]. In this paper, the discontinuous sign function or the saturation function is contained in the first time derivatives of the control input, as shown in *equations (22) and (27)*. The continuous control input shown in *equation (21)* is obtained after integration, thus eliminating the chattering phenomenon without degrading system robustness.

Remark 3.3. The direct measurement of the time derivative of the sliding manifold s_p is sensitive to high-frequency noise, which may magnify noise and deteriorate the control performance. To acquire the time derivative of the sliding manifold s_p in real time, a high-order sliding mode differentiator is introduced as follows [38]:

$$\begin{cases} \dot{z}_0 = v_0 = z_1 - \omega_2 L_1^{0.5} |z_0 - s_p|^{0.5} \text{sign}(z_0 - s_p) \\ \dot{z}_1 = -\omega_1 L_1 \text{sign}(z_1 - v_0) \end{cases} \tag{41}$$

where z_1 and z_2 are the state variables of the differentiator, $\omega_1 > 0$ and $\omega_2 > 0$ are design parameters, and L_1 is a positive constant satisfying $|s_p| < L_1$. Not that the state variable z_1 would converge to the true value of $\dot{s}_p$ in a finite time.

4. Simulation studies

For the purpose of verifying the proposed ASONTSMC scheme, simulation studies comparing the proposed ASONTSMC scheme with a PID controller, a super twisting sliding mode controller (STSMC), and a disturbance observer-based adaptive sliding mode controller (DO-ASMC) are conducted using MATLAB/Simulink in this section. The nominal parameters for the nuclear reactor system adopted in this study are described in Table 1. The change of the desired power P_d of the nuclear reactor system is shown in Fig. 1. It is obvious that the desired power P_d changes from 900 MW → 500 MW with the rate of 2 MW/min.

The design parameters of the ASONTSMC scheme are chosen as follows: $c = 0.7$, $p = 5$, $q = 3$, $k_1 = 0.000003$, $k_2 = 0.0002$, $k_3 = 1500$, $\kappa_0 = 2$, $\kappa_1 = 2$, $\kappa_2 = 2$, $\kappa_3 = 5$, $\kappa_4 = 2$, $\kappa_5 = 2$, $\hat{v}_0(0) = 0.0005$, $\hat{v}_1(0) = 0.0002$, $\hat{v}_2(0) = 0.0001$, $\hat{v}_3(0) = 0.0004$, $\hat{v}_4(0) = 0.0002$, and $\hat{v}_5(0) = 0.006$. These parameters are chosen by a trial-by-trial selection to improve the control performance of the proposed ASONTSMC scheme as much as possible. The proportional, integral, and derivative gains for the closed-loop PID controller are chosen as: $K_P = 5$, $K_I = 0.1$, and $K_D = 0.08$, respectively. The PID gains are determined by trial and error in terms of Ziegler-Nichols step response method [39]. In addition, the lumped disturbances d are assumed as follows:

$$d = -0.1\sin(0.03t) + 0.25\cos\left(0.1t + \frac{\pi}{7}\right) \tag{42}$$

Although the control error would exponentially converge to zero with the proposed ASONTSMC scheme, it is under the assumption that an arbitrarily large input signal can be produced by the proposed controller. To emulate real operation conditions, the physical limitation of the control rod speed is set as $|Z_r| \leq 0.3$ for all controllers. Therefore, the simulation results are a trade-off between the actuator limitation and the control accuracy.

Table 1
Parameter values of the nuclear reactor model [35].

Parameter	Value	Units
P_0	900	MW
β_1	0.000247	–
β_2	0.001385	–
β_3	0.001222	–
β_4	0.002645	–
β_5	0.0008325	–
β_6	0.000169	–
λ_1	0.0124	s^{-1}
λ_2	0.0305	s^{-1}
λ_3	0.111	s^{-1}
λ_4	0.301	s^{-1}
λ_5	1.14	s^{-1}
λ_6	3.01	s^{-1}
Λ	0.08	s
f_f	0.92	–
Ω	6.6	MW/°C
μ_c	71.8	MW.s/°C
μ_f	26.3	MW.s/°C
α_f	-3.24×10^{-5}	$^\circ C^{-1}$
α_c	-2.13×10^{-4}	$^\circ C^{-1}$
M	102	MW.s/°C
G_r	0.02	m^{-1}

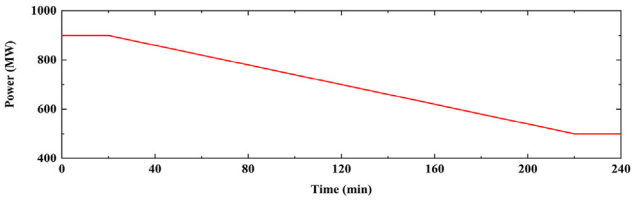

Fig. 1. The change of the desired power P_d of the NPP.

To further quantitatively evaluate the transient and steady-state power-level control performance of the nuclear reactor system as well as the energy consumption, the maximum absolute error (MAE), the integral absolute error (IAE), and the integral absolute control input (IACI) are utilized for fair comparisons. These indices are defined as follows:

$$\text{MAE} = \max_{t \in [0,T]} |e_p(t)| \tag{43}$$

$$\text{IAE} = \int_0^T |e_p(t)| dt \tag{44}$$

$$\text{IACI} = \int_0^T |Z_r(t)| dt \tag{45}$$

where T represents the total simulation time.

The simulation results are presented in Table 2 and Figs. 2–8. Table 2 gives the quantitative power-level control performance comparisons among the ASONTSMC scheme, the PID controller, the STSMC, and the DO-ASMC. The power errors of the nuclear reactor system under the action of the ASONTSMC scheme, the PID controller, the STSMC, and the DO-ASMC are shown in Figs. 2–5, respectively. Fig. 6 plots the control rod speeds produced by the ASONTSMC scheme, the PID controller, the STSMC, and the DO-ASMC. From Table 2 and Figs. 2–5, it is evident that the proposed ASONTSMC scheme exhibits better power-level control performance than the PID controller, the STSMC, and the DO-ASMC. Precisely, the MAE and IAE of the ASONTSMC scheme reach up to 3.1894×10^{-6} and 7.8565×10^{-7}, respectively. By contrast, the MAE and the IAE, respectively, reach up to 0.134 and 14.501 with the PID controller, 0.5089 and 5.2342 with the STSMC, and 1.9999×10^{-3} and 6.9461×10^{-5} with the DO-ASMC, which reveals the superiority of the proposed ASONTSMC scheme. On the other hand, it also can be seen from Table 2 that the ASONTSMC scheme produces less energy consumption than the PID controller, the STSMC, and the DO-ASMC. The IACI of the ASONTSMC scheme reaches up to 20.485, while the IACIs of the PID controller, the STSMC, and the DO-ASMC reach up to 20.486, 20.634, and 20.494, respectively. This indicates the proposed ASONTSMC scheme outperforms the PID controller,

Table 2
Performance comparisons among ASONTSMC, PID controller, STSMC, and DO-ASMC.

Indices	ASONTSMC	PID controller	STSMC	DO-ASMC
MAE	3.1894×10^{-6}	0.1340	0.5089	1.9999×10^{-3}
IAE	7.8565×10^{-7}	14.5010	5.2342	6.9461×10^{-5}
IACI	20.4850	20.4860	20.6340	20.4940

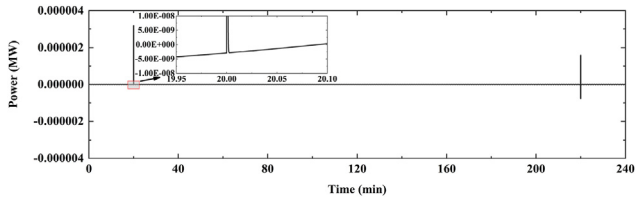

Fig. 2. The power error e_p for the ASONTSMC scheme.

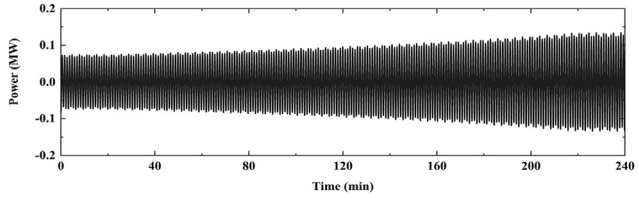

Fig. 3. The power error e_p for the PID controller.

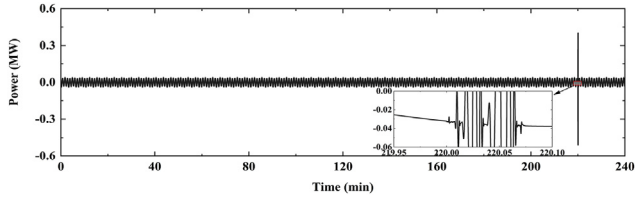

Fig. 4. The power error e_p for the STSMC.

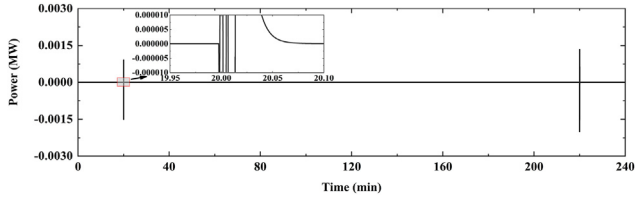

Fig. 5. The power error e_p for the DO-ASMC.

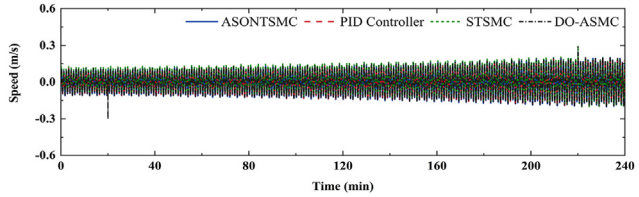

Fig. 6. The control rod speeds produced by the ASONTSMC, the PID controller, the STSMC, and the DO-ASMC.

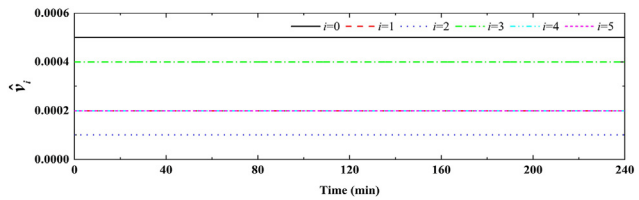

Fig. 7. The changes of the parameters $\widehat{v}_i$ $(i=0,1,2,3,4,5)$ by using the ASONTSMC scheme.

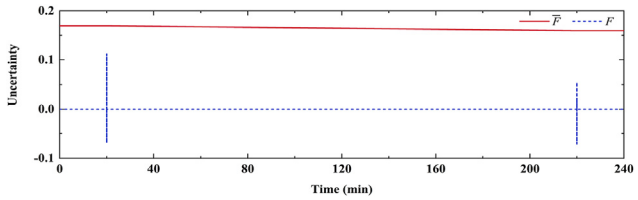

Fig. 8. The changes of the lumped uncertainty F and its estimated upper bound $\overline{F}$ by using the ASONTSMC scheme.

the STSMC, and the DO-ASMC from the points of transient and steady-state power-level control performance, robustness against model uncertainties and external disturbances, and energy consumption. Moreover, it can be clearly observed from Fig. 6 that there exists the actuator saturation phenomenon by using the STSMC and the DO-ASMC. This phenomenon may deteriorate their power-level control performance and even cause the closed-loop control system failure.

The changes of the parameters $\widehat{v}_i$ $(i=0,1,2,3,4,5)$ by using the ASONTSMC scheme are shown in Fig. 7. From this figure, it is clear that the values of parameters $\widehat{v}_i$ $(i=0,1,2,3,4,5)$ are almost unchanged during the power changes from 900 MW → 500 MW. This is because the power error e_p of the nuclear reactor system is exceedingly small under the action of the ASONTSMC scheme, which leads to the first time derivatives of the parameters $\widehat{v}_i$ $(i=0,1,2,3,4,5)$ shown in equation (25) are also exceedingly small. The changes of the lumped uncertainty F and its estimated upper bound $\overline{F}$ by using the ASONTSMC scheme are shown in Fig. 8. One can find that the estimated upper bound F is always greater than the lumped uncertainty F, revealing that the selected parameters are reasonable in simulations.

5. Conclusions

For the power-level control problem of a NPP suffering from lumped disturbances, an ASONTSMC scheme is proposed by combining a PDSM manifold with a NTSM manifold in this paper. In the control framework, the lumped uncertainties are explicitly addressed by means of an adaptive mechanism, in which there is no need for any prior knowledge of the lumped uncertainties. Meanwhile, since the sign function is contained in the first derivative of the control rod speed, the continuous input is obtained after integration such that the chattering effects is alleviated without degrading system robustness. The simulation results reveal that compared with a PID controller, a STSMC, and a DO-ASMC, the proposed ASONTSMC scheme exhibits better control performance and smaller energy consumption. Extending the developed control scheme to the nuclear reactor system with actuator saturation stands for an interesting but challenging task for our future work.

Declaration of competing interest

The authors declare that they have no known competing financial interests or personal relationships that could have appeared to influence the work reported in this paper.

Acknowlegdements

This study is supported by the Open Project Program of the State Key Laboratory of Nuclear Power Safety Monitoring Technology and Equipment of China (Grant No. K-A2020.403).

References

[1] Salah Ud-Din Khan, Ashfaq Ahmad, Testing the pollution haven hypothesis on the pathway of sustainable development: accounting the role of nuclear energy consumption, Nucl. Eng. Technol. 53 (8) (2021) 2746–2752.

[2] Kwangil Kim, Elasticity of substitution of renewable energy for nuclear power: evidence from the Korean electricity industry, Nucl. Eng. Technol. 51 (6) (2019) 1689–1695.

[3] Nasir Mahmood, Zhaohua Wang, Bin Zhang, et al., The role of nuclear energy in the correction of environmental pollution: evidence from Pakistan, Nucl. Eng. Technol. 52 (6) (2020) 1327–1333.

[4] Fabienne Gralla, David J. Abson, Anders P. Møller, Daniel J. Lang, Henrik von Wehrden, Energy transitions and national development indicators: a global review of nuclear energy production, Renew. Sustain. Energy Rev. 70 (2017) 1251–1265.

[5] M. Zarei, R. Ghaderi, N. Kojuri, A. Minuchehr, Robust PID control of power in lead cooled fast reactors: a direct synthesis framework, Ann. Nucl. Energy 102 (2017) 200–209.

[6] Cheng Liu, Jin-Feng Peng, Fu-Yu Zhao, Chong Li, Design and optimization of fuzzy-PID controller for the nuclear reactor power control, Nucl. Eng. Des. 239 (11) (2009) 2311–2316.

[7] Seyed Mohammad Hossein Mousakazemi, Navid Ayoobian, Gholam Reza Ansarifar, Control of the reactor core power in PWR using optimized PID controller with the real-coded GA, Ann. Nucl. Energy 118 (2018) 107–121.

[8] Man Gyun Na, Dong Won Jung, Sun Ho Shin, Jin Wook Jang, Ki Bog Lee, Yoon Joon Lee, A model predictive controller for load-following operation of PWR reactors, IEEE Trans. Nucl. Sci. 52 (4) (2005) 1009–1020.

[9] Jiuwu Hui, Jun Ling, Jingqi Yuan, HGO-based adaptive super-twisting sliding mode power level control with prescribed performance for modular high-temperature gas-cooled reactors, Ann. Nucl. Energy 143 (2020) 107416.

[10] Saeed Saadatzi, Gholamreza Ansarifar, Robust observer-based non-linear control for PWR nuclear reactors with bounded xenon oscillations during load-following operation using two-point nuclear reactor model, Int. J. Nucl. Energy Sci. Technol. 11 (1) (2017) 22–55.

[11] Ramazan Coban, Power level control of the TRIGA Mark-II research reactor using the multifeedback layer neural network and the particle swarm optimization, Ann. Nucl. Energy 69 (2014) 260–266.

[12] Saptarshi Das, Indranil Pan, Shantanu Das, Fractional order fuzzy control of nuclear reactor power with thermal-hydraulic effects in the presence of random network induced delay and sensor noise having long range dependence, Energy Convers. Manag. 68 (2013) 200–218.

[13] Jiuwu Hui, Jun Ling, Jingqi Yuan, Fuzzy adaptive backstepping load following control for MHTGRs with power error constraint and output disturbances, Ann. Nucl. Energy 154 (2021) 108081.

[14] Ehsan Hatami, Salarieh Hassan, Naser Vosoughi, Design of a fault tolerated intelligent control system for a nuclear reactor power control: using extended kalman filter, J. Process Control 24 (7) (2014) 1076–1084.

[15] G. Datatreya Reddy, Youngjin Park, Bijnan Bandyopadhyay, A.P. Tiwari, Discrete-time output feedback sliding mode control for spatial control of a large PHWR, Automatica 45 (9) (2009) 2159–2163.

[16] Nafiseh Zare Davijani, Gholamreza Jahanfarnia, Amir Esmaeili Abharian, Nonlinear fractional sliding mode controller based on reduced order FNPK model for output power control of nuclear research reactors, IEEE Trans. Nucl. Sci. 64 (1) (2016) 713–723.

[17] Guoxu Wang, Jie Wu, Bifan Zeng, Zhibin Xu, Xiaoqian Ma, A nonlinear adaptive sliding mode control strategy for modular high-temperature gas-cooled reactors, Prog. Nucl. Energy 113 (2019) 53–61.

[18] Zhihong Man, Andrew P. Paplinski, Hong Ren Wu, A robust mimo terminal sliding mode control scheme for rigid robotic manipulators, IEEE Trans. Automat. Control 39 (12) (1994) 2464–2469.

[19] Yu Tang, Terminal sliding mode control for rigid robots, Automatica 34 (1) (1998) 51–56.

[20] Yong Feng, Xinghuo Yu, Zhihong Man, Non-singular terminal sliding mode control of rigid manipulators, Automatica 38 (12) (2002) 2159–2167.

[21] Syuan-Yi Chen, Faa-Jeng Lin, Robust nonsingular terminal sliding-mode control for nonlinear magnetic bearing system, IEEE Trans. Control Syst. Technol. 19 (3) (2010) 636–643.

[22] Jin Young Cho, Tae Young Han, Ho Jin Park, Ser Gi Hong, Hyun Chul Lee, Improvement and verification of the DeCART code for HTGR core physics analysis, Nucl. Eng. Technol. 51 (1) (2019) 13–30.

[23] Edward M. Duchnowski, Robert F. Kile, Lance L. Snead, Jason R. Trelewicz, Nicholas R. Brown, Reactor performance and safety characteristics of two-phase composite moderator concepts for modular high temperature gas cooled reactors, Nucl. Eng. Des. 368 (2020) 110824.

[24] Zhe Dong, Yifei Pan, Zuoyi Zhang, Yujie Dong, Xiaojin Huang, Dynamical modeling and simulation of the six-modular high temperature gas-cooled reactor plant HTR-PM600, Energy 155 (2018) 971–991.

[25] M.H.Z. yeganeh, G.R. Ansarifar, Estimation of the poisons reactivity in the PWR nuclear reactors using modified higher order sliding mode observer based on the multi-point nuclear reactor model, Ann. Nucl. Energy 112 (2018) 158–169.

[26] Feng-yu Li, Zhi Chen, Ying Liu, Research on stability of a reactor with power reactivity feedback, Prog. Nucl. Energy 67 (2013) 15–17.

[27] Farrokh Khoshahval, Abdol Aziz Ahdavi, Determination of the maximum speed of WWER-1000 nuclear reactor control rods, Ann. Nucl. Energy 87 (2016) 58–68.

[28] Nafiseh Zare, Gholamreza Jahanfarnia, Abdollah Khorshidi, Jamshid Soltani, Robustness of optimized FPID controller against uncertainty and disturbance by fractional nonlinear model for research nuclear reactor, Nucl. Eng. Technol. 52 (9) (2020) 2017–2024.

[29] Günyaz Ablay, A modeling and control approach to advanced nuclear power plants with gas turbines, Energy Convers. Manag. 76 (2013) 899–909.

[30] Jiuwu Hui, Jingqi Yuan, Disturbance observer-based robust backstepping load-following control for MHTGRs with actuator saturation and disturbances, Nucl. Eng. Technol. 53 (11) (2021) 3685–3693.

[31] Debayan Bose, Shohan Banerjee, M. Kumar, P.P. Marathe, Siddhartha Mukhopadhyay, Amitava Gupta, An interval approach to nonlinear controller design for load-following operation of a small modular pressurized water reactor, IEEE Trans. Nucl. Sci. 64 (9) (2017) 2474–2488.

[32] M. Elsisi, H. Abdelfattah, New design of variable structure control based on lightning search algorithm for nuclear reactor power system considering load-following operation, Nucl. Eng. Technol. 52 (3) (2020) 544–551.

[33] Piyush V. Surjagade, S.R. Shimjith, A.P. Tiwari, Second order integral sliding mode observer and controller for a nuclear reactor, Nucl. Eng. Technol. 52 (3) (2020) 552–559.

[34] Isidori Alberto, Nonlinear Control Systems, Springer Science & Business Media, 2013.

[35] Jiuwu Hui, Jingqi Yuan, Disturbance observer based adaptive sliding mode control for power tracking of PWRs, Nucl. Eng. Technol. 52 (2020) 2522–2534.

[36] Jiuwu Hui, Jingqi Yuan, RBF-based adaptive sliding mode controller with extended state observer for load following of nuclear power plant, Nucl. Eng. Des. 360 (2020) 110465.

[37] Vadim I. Utkin, Sliding Modes in Control and Optimization, Springer Science & Business Media, 2013.

[38] Arie Levant, Higher-order sliding modes, differentiation and output-feedback control, Int. J. Control 76 (9–10) (2003) 924–941.

[39] Karl Johan Åström, Tore Hägglund, Revisiting the Ziegler–Nichols step response method for PID control, J. Process Control 14 (6) (2004) 635–650.